Molecular Biology of the Cell
Vol. 16, 584–596, February 2005

Analysis of Mutant Phenotypes and Splicing Defects Demonstrates Functional Collaboration between the Large and Small Subunits of the Essential Splicing Factor U2AF In Vivo

Christopher J. Webb, Sujata Lakhe-Reddy, Charles M. Romfo, and Jo Ann Wise*

Department of Molecular Biology and Microbiology, School of Medicine, Case Western Reserve University, Cleveland, OH 44106-4960

Submitted September 2, 2004; Revised November 3, 2004; Accepted November 9, 2004
Monitoring Editor: Marvin P. Wickens

The heterodimeric splicing factor U2AF plays an important role in 3′ splice site selection, but the division of labor between the two subunits in vivo remains unclear. In vitro assays led to the proposal that the human large subunit recognizes 3′ splice sites with extensive polypyrimidine tracts independently of the small subunit. We report in vivo analysis demonstrating that all five domains of spU2AF^{LG} are essential for viability; a partial deletion of the linker region, which forms the small subunit interface, produces a severe growth defect and an aberrant morphology. A small subunit zinc-binding domain mutant confers a similar phenotype, suggesting that the heterodimer functions as a unit during splicing in *Schizosaccharomyces pombe*. As this is not predicted by the model for metazoan 3′ splice site recognition, we sought introns for which the spU2AF^{LG} and spU2AF^{SM} make distinct contributions by analyzing diverse splicing events in strains harboring mutations in each partner. Requirements for the two subunits are generally parallel and, moreover, do not correlate with the length or strength of the 3′ pyrimidine tract. These and other studies performed in fission yeast support a model for 3′ splice site recognition in which the two subunits of U2AF functionally collaborate in vivo.

INTRODUCTION

The removal of noncoding introns and the joining of coding exons via splicing, an essential step in the eukaryotic pre-mRNA processing pathway, requires accurate splice site selection by the spliceosome. Initial recognition of the 5′ exon/intron boundary is achieved via base pairing with the U1 snRNA component of the U1 snRNP (Zhuang and Weiner, 1986), whereas U2AF (U2 snRNP auxiliary factor) is the first factor bound to the 3′ splice site (Ruskin *et al.*, 1988). Biochemical complementation assays demonstrated that U2AF is required for the subsequent ATP-dependent association of U2 snRNP with pre-mRNA branchpoints (Ruskin *et al.*, 1988; Valcarcel *et al.*, 1996). Purified U2AF is a heterodimer composed of large and small subunits in humans (Zamore and Green, 1989), *Drosophila melanogaster* (Kanaar *et al.*, 1993; Rudner *et al.*, 1996), *Caenorhabditis elegans* (Zorio *et al.*, 1997; Zorio and Blumenthal, 1999) and *Schizosaccharomyces pombe* (Potashkin *et al.*, 1993; Wentz-Hunter and Potashkin, 1996). Functional conservation of this splicing factor is evidenced by 1) the restoration of splicing activity to U2AF-depleted HeLa nuclear splicing extracts via addition of *Drosophila* U2AF large subunit (dmU2AF^{LG}; Zamore and Green, 1991) and 2) the ability of human U2AF^{35} (hsU2AF^{SM}) to restore growth to an *S. pombe* strain lacking the small subunit (Webb and Wise, 2004).

The structural domains of U2AF are also conserved except in *Saccharomyces cerevisiae*, where the large subunit is highly divergent and the small subunit is absent entirely (Abovich *et al.*, 1994). The small subunit of U2AF consists of two zinc-binding domains (ZBDs) surrounding a central pseudo-RNA recognition motif (ΨRRM; Rudner *et al.*, 1998b), also known as a PUMP (PUF60/U2AF/MUD2 protein-protein interaction) domain (Page-McCaw *et al.*, 1999) or a UHM (U2AF homology motif; Kielkopf *et al.*, 2004), which are highly conserved between *S. pombe* and humans, followed by a C-terminal domain that consists of RS or RS/glycine repeats in metazoan orthologues, which are not present in the fission yeast protein. We recently demonstrated that the three conserved domains including both ZBDs and the ΨRRM of *S. pombe* U2AF small subunit (spU2AF^{SM}) contribute to RNA binding and are essential for function in vivo, whereas the more divergent C-terminal domain is dispensable (Webb and Wise, 2004). A comparable domain ablation analysis in vivo has not been carried out for the U2AF large subunit, which consists of an N-terminal RS domain, a linker region, two classical RRMs (RNA recognition motifs) and a ΨRRM (Zamore *et al.*, 1992). Such an analysis would complement extensive biochemical data demonstrating that this subunit is the major contributor to RNA binding (Rudner *et al.*, 1998a; Wu *et al.*, 1999; Kielkopf *et al.*, 2001) and interacts with multiple protein partners implicated in splicing including p54 (Zhang and Wu, 1996), UAP56 (Fleckner *et al.*, 1997), Sip1 (Zhang and Wu, 1998), SF1/BBP (Berglund *et al.*, 1998), and SAP155 (Gozani *et al.*, 1998), as well as nonsplicing factors such as WT1 (Davies *et al.*, 1998) and poly(A) polymerase (Vagner *et al.*, 2000).

Article published online ahead of print in *MBC in Press* on November 17, 2004 (http://www.molbiolcell.org/cgi/doi/10.1091/mbc.E04-09-0768).

* Corresponding author. E-mail address: jaw17@case.edu.

Abbreviations used: U2AF^{SM}, U2AF small subunit; U2AF^{LG}, U2AF large subunit; SF1/BBP, splicing factor 1/branchpoint bridging protein; ΨRRM, pseudo-RNA recognition motif.

RNA-binding assays (Zamore *et al.*, 1992; Rudner *et al.*, 1998a) and in vitro selection studies (Singh *et al.*, 1995; Wu *et al.*, 1999; Banerjee *et al.*, 2004) demonstrated that the large subunit of U2AF interacts with the 3′ polypyrimidine tract, whereas the small subunit functions in recognition of the 3′ AG dinucleotide (Merendino *et al.*, 1999; Wu *et al.*, 1999; Zorio and Blumenthal, 1999b). The bipartite nature of the RNA target sequences for the two subunits, in combination with biochemical complementation data demonstrating that addition of the human large subunit (hsU2AF^{LG}) alone to U2AF-depleted HeLa nuclear extracts can rescue splicing of substrates that contain long polypyrimidine tracts (Wu *et al.*, 1999; Guth *et al.*, 2001), led to a widely accepted model for 3′ splice site recognition by U2AF. The central tenet of this model is that the binding energy contributed by the small subunit/AG interaction is essential only for introns with less extensive polypyrimidine tracts (reviewed in Moore, 2000), consistent with earlier splicing assays of mutant human pre-mRNAs in vitro, which indicated that the requirement for a 3′ AG to proceed through the first step of splicing (AG-dependence) could be eliminated by expanding the polypyrimidine tract (Reed, 1989). In *S. pombe*, mutating the terminal AG dinucleotide prevented the first transesterification reaction for all three introns examined (Romfo and Wise, 1997), as for a subset of mammalian pre-mRNAs (Reed, 1989; Wu *et al.*, 1999). However, doubling the length of the polypyrimidine tract in two different fission yeast introns did not render the AG dinucleotide dispensable in vivo (Romfo and Wise, 1997), providing the first hint that both subunits of U2AF may be important for initial recognition of a broad spectrum of introns in this organism.

In this report, we demonstrate that *S. pombe* U2AF large subunit (spU2AF^{LG}) mutants lacking the linker region or any of the C-terminal RRMs or ΨRRM are recessive lethal, whereas deleting the N-terminal RS domain confers dominant lethality. A partial deletion of the spU2AF^{LG} linker, which interacts with the small subunit in *S. pombe* (Wentz-Hunter and Potashkin, 1996) as well as humans (Zhang *et al.*, 1992; Kielkopf *et al.*, 2001) and *Drosophila* (Rudner *et al.*, 1998c), produces an unusual branched morphology that is also observed in a triple substitution within the second zinc-binding domain of spU2AF^{SM}. As the aberrant morphology is likely to reflect a common underlying splicing defect, this result, in conjunction with our previous data (Romfo and Wise, 1997), prompted us to ask whether splicing of different introns in vivo requires parallel contributions from the two subunits of spU2AF. Analysis of 22 diverse pre-mRNAs after separate mutational inactivation of each subunit reveals that those introns that are most highly dependent on spU2AF^{LG} also exhibit a marked dependence on spU2AF^{SM}. Moreover, counter to what would be predicted from the model for metazoan U2AF function (Moore, 2000), the length and sequence of the polypyrimidine tract do not correlate with the requirement for either subunit. In addition to explaining our previous finding that expanding the polypyrimidine tract did not negate the requirement for the AG dinucleotide, these results are consistent with the recent demonstration that, in *S. pombe*, most of the U2AF heterodimer is maintained in a tight complex with SF1/BBP, apparently optimized to recognize the branchpoint/3′ splice site region as a functional unit (Huang *et al.*, 2002).

MATERIALS AND METHODS

Plasmid Construction and Mutagenesis

All oligonucleotides used in this study are listed in Table 1. spU2AF^{LG} mutants were generated using either site-directed mutagenesis of single-stranded DNA (ΔL3-P102; ΔD2-P140; ΔP139-P189; F247D, I249D; F353, F355D; F476D, Y479D) using commercially available reagents (Amersham, Arlington Heights, IL) with oligonucleotides 1–6 (Table 1) or by overlap extension PCR (ΔP124-P189; W135F; W135A) using Platinum *pfx* DNA polymerase (Invitrogen, Carlsbad, CA) with the flanking primers prp-Nde and prp-Bam (Romfo *et al.*, 1999) in combination with appropriate internal primers (9–14) listed in Table 1. Mutants generated by overlap extension PCR were subcloned into the *S. pombe* plasmid *prp2*+/PIRT3 (Romfo *et al.*, 1999) as *Nru*I-*Nhe*I or *Bgl*II fragments. The presence of each mutation was confirmed by DNA sequencing (Cleveland Genomics, Cleveland, OH). Two-hybrid alleles were constructed by amplification of spU2AF^{LG} mutant templates with the primers prp-Nde and prp-Bam (Romfo *et al.*, 1999) and oligonucleotides 7 and 8. The resulting fragments were inserted into pAS2–1 (BD Sciences Clontech, Palo Alto, CA) and sequenced. To express a fragment derived from the β-globin 3′ intron/exon boundary (Wu *et al.*, 1999) in the modified three-hybrid system (Webb and Wise, 2004), the 5′ phosphorylated oligonucleotides 15 and 16 were annealed and inserted into the *Xma*I and *Cla*I sites of p4130 (kindly provided by John Woolford, Carnegie Mellon University; described in Fewell and Woolford, 1999) to generate the plasmid β-globin/pIII MS2–1 B,H,C.

Two-hybrid Analysis

To analyze heterodimer formation, mutant alleles of *uaf1*$^+$ (spU2AF^{LG}) were expressed in pAS2–1, as noted above, and the interacting partner, wild-type *uaf2*$^+$ (spU2AF^{SM}), was expressed in pACT2 (James *et al.*, 1996). Two-hybrid analysis was performed as previously described (Webb and Wise, 2004). Briefly, the fusion protein constructs were cotransformed into the *S. cerevisiae* strain PJ69–4A (*MAT*a *trp*1-901 *leu*2-3112 *ura*3-52 *his*3-200 *gal*4Δ *gal*80Δ *LYS*2::*GAL*1-*HIS*3 *GAL*2-*ADE*2 *met*2::*GAL*7-*lacZ*; 20) as described (James *et al.*, 1996) except that dimethyl sulfoxide was added to the final incubation step.

Three-hybrid Analysis

Three-hybrid assays to measure RNA-protein interactions were conducted as described previously (Webb and Wise, 2004). Briefly, one plasmid carrying either the large subunit gene or the large and small subunit genes and another expressing a hybrid RNA containing a human β-globin 3′ splice site were cotransformed into the L40 *S. cerevisiae* strain (*MAT*a *ura*3-52 *le*u2-3112 *his*3Δ200 *trp*1Δ1 *ade*2 *LYS*2::(lexAop)-HIS3 *ura*3::(lexAop)-*lacZ*; 44), kindly provided by Dr. J. Woolford. Duplicate transformants were grown to midlog phase and replica plated onto media containing varying amounts of 3-aminotriazole (3-AT). Plate assays were reproducible, with visually indistinguishable results.

Phenotypic Analysis in S. pombe

The ability of large subunit mutants to support growth was determined using the complementation assay previously described in the strain SpCr1, which is heterozygous for deletion of the gene encoding spU2AF^{LG} (Romfo *et al.*, 1999). Dominant negative effects of large subunit mutants were performed as described earlier (Romfo *et al.*, 1999).

To examine the morphology of spU2AF subunit mutants, microscopy was performed with exponentially growing cells using a Zeiss (Jena, Germany) Axioplan-2 microscope equipped with Nomarski differential interference (DIC) optics, a plan-NEOFLUAR (100×, numerical aperture 1.3) oil immersion objective and a Hamamatzu (Tokyo, Japan) C4742–95 progressive scan cooled charge-coupled device camera. Images were captured with QED acquisition software.

RNA Preparation and Analysis

To assay for splicing defects, the temperature-sensitive (ts) mutants spU2AF^{SM} [Y108A, F111A] and spU2AF^{LG} C387Y and corresponding isogenic wild-type strains were grown in selective media to midlog phase at the permissive temperature (30°C) followed by inoculation of equal aliquots into media prewarmed to 30 or 37°C. After 2 h (2, 4, and 6 h for *ypt5*-I1) at the nonpermissive temperature, cells were harvested and total RNA extracted as previously described (Alvarez *et al.*, 1996). Semiquantitative RT-PCR assays were performed and the results analyzed as in published work (Webb and Wise, 2004) using the primers (17–60) listed in Table 1.

RESULTS

The Dominant Lethality Conferred by U2AF^{LG} RS Domain Deletions Requires Binding to U2AF^{SM}

Two recombinant human U2AF^{LG} mutant proteins carrying deletions in the N-terminal domain were previously analyzed in nuclear splicing extracts from HeLa cells (Valcarcel *et al.*, 1996). In hsU2AF^{LG} Δ1–63, removal of all but one RS/SR dipeptides dramatically reduced the protein's ability to restore splicing activity to an extract depleted of hsU2AF, whereas the more extreme mutant, hsU2AF^{LG} Δ1-94, which

Table 1. Oligonucleotides and primers used in these studies

Oligonucleotide or primer and function	Designation	Sequence
Oligonucleotides for *uaf1+* phosphorothioate-based site-directed mutagenesis		
1	D7RS mut	5′ gcttctttctcggctgggaggcaaatccatgttagtgaat gaatatg 3′
2	D11RS mut	5′ cagcagtaaccaattcataaccaggatccatgttagt gaatgaatatg 3′
3	DHinge	5′ ctagcacctggttgtaagggtggtttaatgtcccataaag a 3′
4	F247D/I249D	5′ cgacctcaagatcagcatcgttttcttctttacag 3′
5	F353D/F355D	5′ aggatttttaaattcgcaatcacaatcacccttcgaagat c 3′
6	F476D/Y479D	5′ gatatcggagtctcgtacatcaacctttccagttc 3′
Oligonucleotides for making two-hybrid constructs		
7	D7RS-Nde	5′ tagaagtccatatggatttgcctcccagccgagaa 3′
8	slrDRS Nde	5′ ggacattaaaccatatggatcctggttatgaattg 3′
Oligonucleotides for *uaf1+* overlap extension PCR mutagenesis		
9	PrpF476AY479Apcrmut1	5′ cgggattaggaactggaaaggttgctgtacgagcttc cgatatcagatctgcagaggtc 3′
10	PrpF476AY479Apcrmut2	5′ aacctttccagttcctaatcccg 3′
11	PrpΔP124-P188pcrmut3	5′ ggaactcgaacaattgagagatgtaacacccttacaac caggtgctagcagac 3′
12	PrpΔP124-P188pcrmut4	5′ tgttacatctctcaattgttcgagttcc 3′
13	Prp2.W135F.1	5′ cagtggaaaaggaagcgctctttatttgacattaaacca cctggttatg 3′
14	Prp2.W135-.2	5′ taaagagcgcttccttttccactg 3′
Oligonucleotides for making RNA three-hybrid construct		
15	β-globin.XmaI.s	5′ ccgggtctcttcctttgtcagggaaatgggaac 3′
16	β-globin.ClaI.as	5′ cggttcccatttccctgacaaaggaagagac 3′
Primers for RT-PCR splicing assays		
17	SPCC16A11.08-I2.exon.2	5′ gatgcgtcggcagtatcccg 3′
18	SPCC16A11.08-I2.exon.3	5′ gaagagcgcaaatgagcgaatgg 3′
19	SPCC830.12-I1.exon1	5′ gaggaccagggtcctctgctg 3′
20	SPCC830.12-I1.exon2	5′ cacagcgaatctttatagtcactg 3′
21	SPAC17A5.16-I3.exon3	5′ ccgttggatgatgaagtttggg 3′
22	SPAC17A5.16-I3.exon4	5′ gtaggcgaatgcagtttaacgc 3′
23	pyp3-I1.exon1	5′ ctcgtgttcgtttagatccaatg 3′
24	pyp3-I1.exon2	5′ ggcgttccctcaatttggtaagc 3′
25	erf1-I2.exon2	5′ ggagatcagctgaaggcttctac 3′
26	erf1-I2.exon3	5′ tacaagcagcatctacacggtcc 3′
27	mcs2-I2.exon2	5′ tttatctaattaactctgtcatggag 3′
28	mcs2-I2.exon3	5′ aggacgaaatggaagccagacg 3′
29	cdc16-I2.exon2	5′ ttattggataaatgccttgaagtcc 3′
30	cdc16-I2.exon3	5′ tcggaaaataaacatttgtgcaatc 3′
31	ypt5-I1.exon1	5′ cttgttgttacactcaaaataaatatggc 3′
32	ypt5-I1.exon2	5′ catcaaattgatctttaacgaatcgaag 3′
33	cdc17-I2.exon2	5′ actagcaaacggttggaaatcattg 3′
34	cdc17-I2.exon3	5′ agctacaagaccaagatcaccaac 3′
35	SPAC22F8.13-I2.exon2	5′ gatcttcctaaaggatcaaggac 3′
36	SPAC22F8.13-I2.exon3	5′ cagttcctaaataaacaaatgcagaac 3′
37	erf1-I4.exon4	5′ cttgccaatatttgtctcattacag 3′
38	erf1-I4.exon5	5′ ggtccttcaaaatttcattaaggg 3′
39	cdc2-I2.exon2	5′ gggaattccatatgttgtcagggcgtattgtg 3′
40	cdc2-I2.exon3	5′ gaaggatccggtaaacttttgaacaagtctc 3′
41	cdc16-I1.exon1	5′ gtgtgtctcaatcgtctctttcac 3′
42	cdc16-I1.exon2	5′ atacgtgtacaaacgatggtcaag 3′
43	pim1-I1.exon1	5′ gaaggtgctttatctcatctacg 3′
44	pim1-I1.exon2	5′ gtagtcaaggcaataatatggtcc 3′
45	rad9-I3.exon3	5′ gatggcagcacagttcaacacc 3′
46	rad9-I3.exon4	5′ aagaacaatgattgaccagcatcg 3′
47	pck1-I1.exon1	5′ gcaagctttcaaactagtaccagg 3′
48	pck1-I1.exon2	5′ tcgtatatgaccatcaggacaaag 3′
49	rad26-I2.exon2	5′ aatcccaagaatcactcatgcaac 3′
50	rad26-I2.exon3	5′ agtccgatgcatactattaaggg 3′
51	top1-I2.exon2	5′ gaaggaggcaaagacgcggttc 3′
52	top1-I2.exon3	5′ ccaccatttcccattactttagc 3′
53	cdc16-I3.exon3	5′ ttaccatatgggatttttgtttgc 3′
54	cdc16-I3.exon4	5′ cagaacaccagcttcagaatcc 3′
55	chk1-I3.exon3	5′ caccttgggatgaagcaattagc 3′
56	chk1-I3.exon4	5′ tagttcgaaatggtgtacttgagg 3′
57	erf1-I3.exon3	5′ atgggatcctaccataccttgg 3′
58	erf1-I3.exon4	5′ gtcccctctccgtttccttgg 3′
59	swi4-I1.exon1	5′ cgatctcgaaaagggtctgtcc 3′
60	swi4-I1.exon2	5′ accttgttgttattttcagcttctttttg 3′

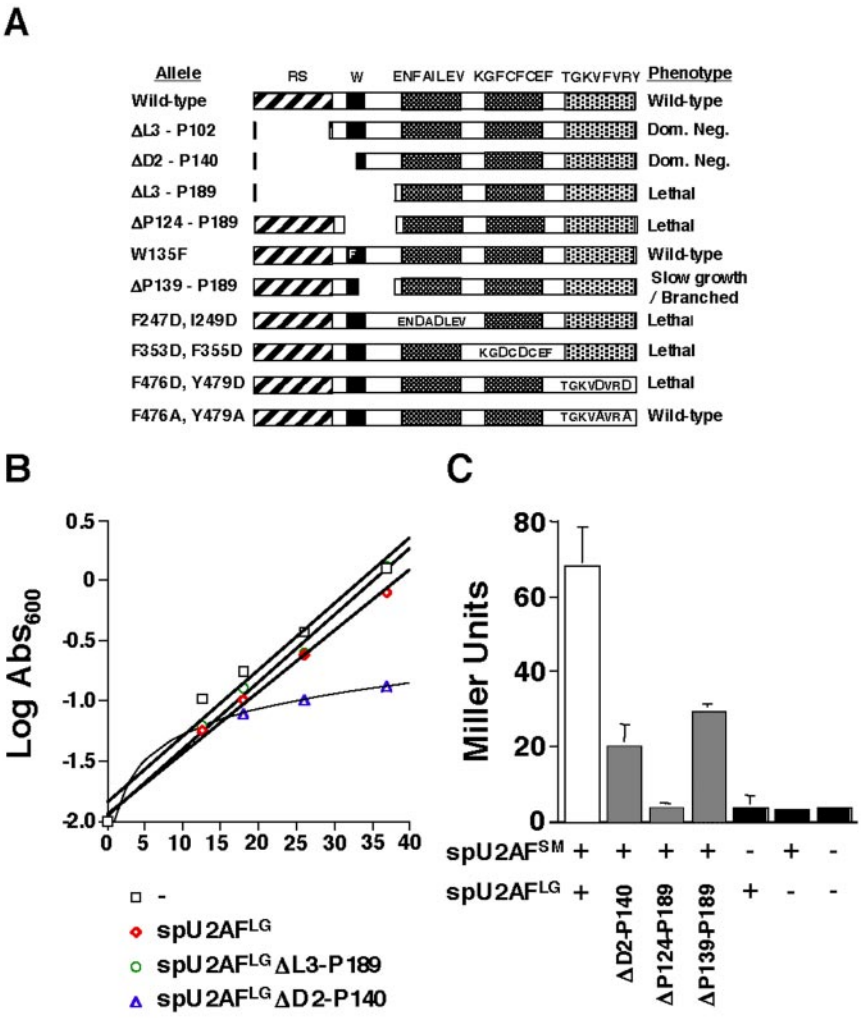

Figure 1. Domain structure of spU2AF^{LG} and mutant phenotypes. (A) The relative lengths and positions of the conserved domains of spU2AF^{LG} are depicted as rectangles with amino acids or motifs targeted by mutations written above the wild-type schematic. Also included in the figure is the previously described ΔRS/Hinge (ΔL3-P189) mutant (Romfo *et al.*, 1999). RS domain, diagonal stripes; linker region, black with the phenylalanine replacement of the key tryptophan (Kielkopf *et al.*, 2001) shown in white; RRM1 and RRM2, cross-hatched with the RNP-1 motif shown on a white background with mutated amino acids in large type; ΨRRM, stippled with the RNP1-like motif shown on a white background with mutated amino acids in large type. Phenotypes were assessed as described previously (Romfo *et al.*, 1999; Webb and Wise, 2004). (B) Dominant negative effect on growth of overexpressing the ΔD2-P140 allele. A wild-type fission yeast strain (DS2) was transformed with the indicated plasmids in the presence of thiamine to repress the *nmt1* promoter (Romfo *et al.*, 1999). Growth was monitored by measuring absorbance$_{600}$ after a shift to medium lacking thiamine at time 0. In addition to the vector only and wild-type controls, we also analyzed growth of a strain harboring a plasmid carrying the ΔRS/Hinge allele, which we previously showed confers a recessive lethal phenotype (Romfo *et al.*, 1999). (C) Two-hybrid analysis of heterodimer formation in mutants predicted to disrupt the large and small subunit interface. The figure shows the results of β-galactosidase assays, with the data expressed in Miller Units. Error bars, SD for n = 3. Wild-type, white bars; mutants, gray bars; negative controls, black bars.

eliminates the entire RS domain and approximately half of the linker region, displayed no detectable activity in vitro. To assess the role of the N-terminal RS domain in vivo, we analyzed two similar alleles (ΔL3-P102 and ΔD2-P140; Figure 1) of *S. pombe* U2AF^{LG}, which contains the same number of RS/SR dipeptide repeats (10) in the intact N-terminal domain as hsU2AF^{LG}. To avoid structural perturbations, we constructed deletions that extended between two prolines.

Our initial phenotypic analysis suggested that an allele carrying a complete deletion of the N-terminal domain of spU2AF^{LG} (ΔD2-P140; Figure 1A) complements the otherwise lethal *uaf1*::*ura4* gene disruption described earlier (Romfo *et al.*, 1999). However, upon recovery and sequencing of plasmid from the haploid derivatives, we discovered that this allele had in fact been repaired by gene conversion because of dominant negative selective pressure, similar to what we previously found for U1 snRNA mutants (Alvarez *et al.*, 1996). Gene conversion was confirmed by Western blot analysis (unpublished data), which showed that the sole protein expressed in these cells is full-length. The dominant effect of the spU2AF^{LG} ΔD2-P140 allele was unequivocally demonstrated by overexpressing it from the derepressible *nmt1* (no message on thiamine) promoter in an otherwise wild-type *S. pombe* strain. Under derepressing conditions, the presence of the deletion allele nearly abolishes growth as judged by failure to form colonies after streaking (unpublished data) and by growth analysis (Figure 1B). In contrast to cells harboring the vector only or a wild-type control, the strain overexpressing the DRS (ΔD2-P140) allele virtually ceases growth ~12 h after the shift to medium lacking thiamine. Analogous experiments indicate that the less extreme RS domain deletion ΔL3-P102, which retains three RS/SR dipeptides as well as the entire linker region, also dominantly interferes with growth in fission yeast.

Our previous work indicated that a more extensive spU2AF^{LG} deletion (ΔRS/Hinge = ΔL3-P189) lacking the linker region, which has been implicated in small subunit interactions (Zhang *et al.*, 1992; Wentz-Hunter and Potashkin, 1996; Rudner *et al.*, 1998c; Kielkopf *et al.*, 2001), as well as the RS domain, produced recessive lethality (Romfo *et al.*, 1999); these findings are recapitulated in Figure 1, A and B. In light of the contrast with the dominant lethality conferred by the ΔD2-P140 allele, we hypothesized that spU2AF^{SM} plays a role in the dominant negative effects of spU2AF^{LG} deletion mutants. Consistent with this idea, the spU2AF^{LG} ΔP124-P189 mutant, which removes the linker region alone, is recessive lethal (Figure 1A).

The results of two-hybrid assays further support a role for the small subunit in dominant lethality, as the spU2AF^{LG} ΔP124-P189 mutant interacts with spU2AF^{SM} at background levels, whereas the spU2AF^{LG} ΔD2-P140 mutant, in which only the N-terminal portion of the linker is deleted, shows

significant small subunit binding (Figure 1C). Notably, the ΔD2-P140 mutant eliminates the highly conserved tryptophan at position 135, which was proposed based on structural data for a minimal human heterodimer to make a key contact with U2AF^{SM} in a manner dependent on the unique properties of this amino acid (Kielkopf *et al.*, 2001). Consistent with our two-hybrid data, however, we find that an allele carrying a phenylalanine substitution at amino acid 135 of spU2AF^{LG} supports growth of fission yeast (Figure 1A). Although this is a conservative substitution that is also found in both the large and small subunits of plant U2AF orthologues, modeling studies predict that reciprocal changes in the binding pockets coevolved in plants to compensate for the lack of an additional five-membered ring on the phenylalanine side-chains that is present in tryptophan (Kielkopf *et al.*, 2001). In contrast to plants, both subunits of fission yeast U2AF contain tryptophans at the relevant positions and are thus likely to form a tongue-in-groove heterodimeric interface similar to that proposed for the minimal human heterodimer (Kielkopf *et al.*, 2001). This view is bolstered by our finding that human U2AF^{SM} can support *S. pombe* viability in the absence of spU2AF^{SM} (Webb and Wise, 2004). Thus, the phenylalanine substitution is most likely tolerated in spU2AF^{LG} because this amino acid can still be accommodated in the larger binding pocket that normally envelops a tryptophan. Taken together, our data support the idea that both the N-terminal portion of the linker emphasized by in vitro studies and the C-terminal region make substantial contributions to spU2AF function in vivo.

In analyzing the pattern of dominant lethality conferred by large subunit mutations, we also noted that this phenotype arises only when the RS domain is absent. In particular, the spU2AF^{LG} ΔP139-P189 mutant, which removes the C-terminal portion of the linker (Figure 1A), is recessive. The phenotypic consequences of the ΔP139-P189 mutant in *S. pombe* include extremely slow growth and an aberrant morphology (described below), and the encoded protein displays an intermediate level of binding to the small subunit in the two-hybrid system (Figure 1C). In keeping with our data, it was possible to identify alleles carrying multiple point mutations within the linker region of the *Drosophila* U2AF large subunit that compromise, but do not abolish, heterodimer formation in vitro and affect viability of the intact organism (Rudner *et al.*, 1998c). Inactivating substitutions within RRM1, RRM2, and the ΨRRM are recessive lethal.

To determine whether the two canonical RRMs of spU2AF^{LG} are critical for viability, we replaced two large hydrophobic residues within RNP1 of RRM1 or RRM2, which were suggested by modeling to interact with RNA via intercalation (Ito *et al.*, 1999), with aspartates, which are predicted to repel a negatively charged RNA. The [F247D, I249D] double substitution in RRM1 and the [F353D, F355D] RRM2 mutant both produce recessive lethality (Figure 1A), consistent with the complete abolition of RNA-binding activity in vitro conferred by analogous substitutions in the mammalian SR protein ASF/SF2 (Caceres and Krainer, 1993). The lethal effect of mutating either RRM1 or RRM2 indicates that each is independently essential for viability in *S. pombe*, consistent with the finding that both canonical RRMs of hsU2AF^{LG} have RNA-binding activity when tested individually in vitro (Ito *et al.*, 1999).

Recent evidence indicates that deleting the entire ΨRRM of spU2AF^{LG} is lethal in vivo even though the hsU2AF^{LG} ΨRRM does not contribute to RNA binding in vitro (Banerjee *et al.*, 2004). At first pass, our finding that a double aspartate substitution within the RNP1-like sequence, [F476D, Y479D], is lethal (Figure 1A) might seem at odds with the lack of a role in RNA binding, as charged substitutions of large hydrophobic amino acids within RNP1 of canonical RRMs disrupt contacts with RNA (e.g., Caceres and Krainer, 1993). Furthermore, the analogous substitution in the spU2AF^{SM} ΨRRM was also lethal, and our data indicate that this domain does contribute to RNA binding (Webb and Wise, 2004). The discrepancy can be reconciled by structural data implicating the hsU2AF^{LG} amino acid analogous to F476 in packing helix C against the β-sheet that contains the RNP1-like sequence (Selenko *et al.*, 2003), which would block the potential RNA binding surface, whereas the small subunit of U2AF does not have a recognizable helix C (Kielkopf *et al.*, 2001). The inability of the [F476D, Y479D] substitution to support growth also echoes the effect of the corresponding mutation in the ΨRRM of the *S. cerevisiae* large subunit orthologue MUD2. Specifically, MUD2 is essential only when the U1A gene is also deleted, and the synthetic lethality cannot be rescued by an allele carrying a double aspartate substitution in the ΨRRM (Abovich *et al.*, 1994).

Whereas replacement of the large hydrophobic amino acids in the RNP1-like peptide of the *S. pombe* U2AF^{LG} ΨRRM is lethal, a more conservative double alanine substitution is phenotypically silent (Figure 1A). Again, a structural comparison with its human counterpart may help to explain the data, as Y479 of spU2AF^{LG} is likely to contribute a core side-chain that stabilizes the protein fold against helix B. The Y479D mutation may not be tolerated because the charge perturbs the structure, while a more conservative alanine substitution would allow the fold to be retained. In contrast to the [F476A, Y479A] spU2AF^{LG} mutant, the analogous double alanine replacement in the ΨRRM of spU2AF^{SM} leads to temperature-sensitive growth (Webb and Wise, 2004). A likely explanation is that these substitutions disrupt RNA binding.

A Partial Deletion of the U2AF^{LG} Linker Region Confers a Phenotype Similar to a U2AF^{SM} Zinc-binding Domain Mutant

Our mutagenesis strategy, which involved making deletions that extend between prolines, yielded an spU2AF^{LG} allele (ΔP139-P189) that only partially deletes the linker, retaining the twelve N-terminal amino acids of the region defined in an earlier structural study (Kielkopf *et al.*, 2001). As noted above, the spU2AF^{LG} ΔP139-P189 mutant displays a reduced two-hybrid interaction with spU2AF^{SM} (Figure 1C) but does support growth of *S. pombe* (Figure 1A), albeit poorly compared with an isogenic wild-type strain as judged by the dramatically reduced colony size. An even more notable phenotype of the spU2AF^{LG} ΔP139-P189 mutant is that individual cells harboring this deletion allele as their sole source of U2AF large subunit display an aberrant branched morphology (Figure 2, compare A and B). Strikingly, a triple substitution (C157S, C163S, H167I) within the second zinc-binding domain (ZBDII) of the *S. pombe* U2AF small subunit identified in a separate study (Webb and Wise, 2004) also exhibits slow growth and a branched morphology (Figure 2, compare C and D). Like the other 35 small subunit alleles analyzed to date (Webb and Wise, 2004), this mutant is recessive as judged by the reversal of its deleterious effects on introduction of a plasmid-borne wild-type allele. The unusual nature, yet remarkable similarity, of the phenotypes conferred by the spU2AF^{LG} ΔP139-P189 and spU2AF^{SM} [C157S, C163S, H167I] alleles suggest that they may have the same underlying molecular basis.

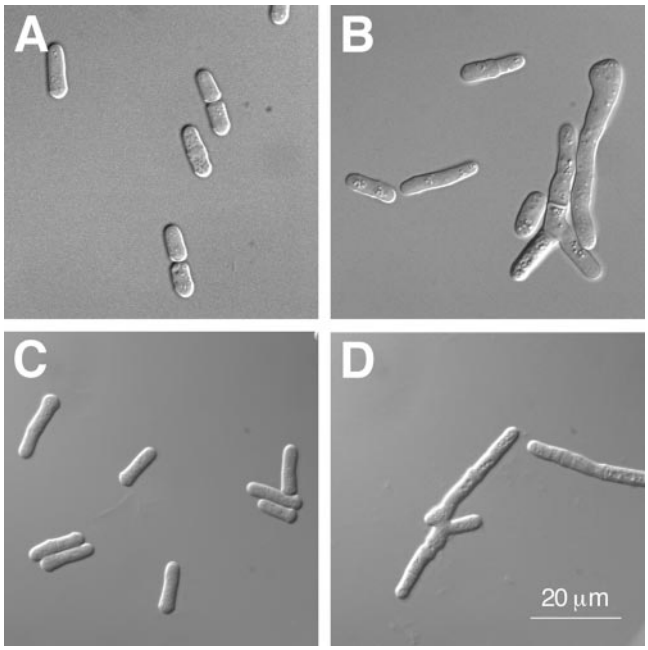

Figure 2. Microscopic analysis of the spU2AF^{LG} ΔP139-P189 and spU2AF^{SM} [C157S, C163S, H167I] mutants. (A) A haploid strain with a plasmid harboring wild-type spU2AF^{LG} covering a disruption of the *uaf1*+ locus (Romfo *et al.*, 1999). (B) A haploid strain with a plasmid harboring the spU2AF^{LG} ΔP139-P189 mutant covering a disruption of the *uaf1*+ locus. (C) A haploid strain with a plasmid harboring wild-type spU2AF^{SM} covering a disruption of the *uaf2*+ locus (Webb and Wise, 2004). (D) A haploid strain with a plasmid harboring the spU2AF^{SM} [C157S, C163S, H167I] mutant covering a disruption of the *uaf2*+ locus. Magnification, ×1000.

As previously characterized *S. pombe* mutants that exhibit a similar pseudohyphal appearance have generally been linked to septation or cytokinetic defects such as cell separation (Le Goff *et al.*, 1999), we tested the three intron-containing pre-mRNAs implicated in these processes for splicing defects in the small subunit pZBDII mutant. Although precursor accumulation was observed, it was not dramatic; most definitively, a cDNA encoding *imp2*, which displayed the most substantial splicing defect, was unable to reverse either the growth defect or the branched morphology (unpublished data). Thus, although we still consider defective splicing of one or more pre-mRNAs that encode gene product(s) required for cytokinesis the most reasonable explanation for the morphology of both the spU2AF^{SM} pZBDII mutant and the spU2AF^{LG} mutant carrying a partial deletion of the linker region, further work will be required to identify the pre-mRNAs whose product(s) have become rate-limiting for growth.

Given that the spU2AF^{LG} mutant carrying a partial deletion of the linker region is defective in heterodimer formation (Figure 1C), we performed two-hybrid analysis on the small subunit ZBDII mutant. As shown in Figure 3A, the [C157S, C163S, H167I] spU2AF^{SM} mutant shows a two-hybrid interaction with spU2AF^{LG} comparable to wild-type, consistent with our previous finding that even lethal amino acid substitutions in either zinc-binding domain did not disrupt large subunit interactions (Webb and Wise, 2004). As noted in the *Introduction*, U2AF function involves formation of a complex between the heterodimer and the bipartite (polypyrimidine tract/AG dinucleotide) 3′ splice site. Defective heterodimer formation by the spU2AF^{LG} ΔP139-P189 mutant is predicted to destabilize this complex and thus disrupt splicing. However, a similar effect could also result from disrupting the interaction of U2AF with the 3′ splice site. We therefore tested whether the [C157S, C163S, H167I] spU2AF^{SM} mutant shows diminished binding to RNA in a modified three-hybrid assay where the large subunit is co-expressed (Figure 3B). Consistent with our previous finding that *S. pombe* U2AF^{SM} ZBD mutations decrease the interaction of the heterodimer with small RNAs carrying 3′ splice sites (Webb and Wise, 2004), the [C157S, C163S, H167I] allele does indeed produce a lower signal in the three-hybrid system (Figure 3B). The most parsimonious interpretation of these data in aggregate is that the molecular defect conferred by both the spU2AF^{LG} linker region deletion and the ZBDII spU2AF^{SM} triple substitution is an unstable complex between the U2AF heterodimer and one or more 3′ splice sites.

The Length and Pyrimidine Content of 3′ Splice Sites Do not Correlate with U2AF Requirements in S. pombe

The correlation between the dominant negative phenotypes of large subunit RS domain deletions and their ability to bind the small subunit (Figure 1) led us to hypothesize that the U2AF heterodimer obligatorily functions as a unit during splicing in *S. pombe*, a view reinforced by the identification of spU2AF^{LG} and spU2AF^{SM} mutants with similar phe-

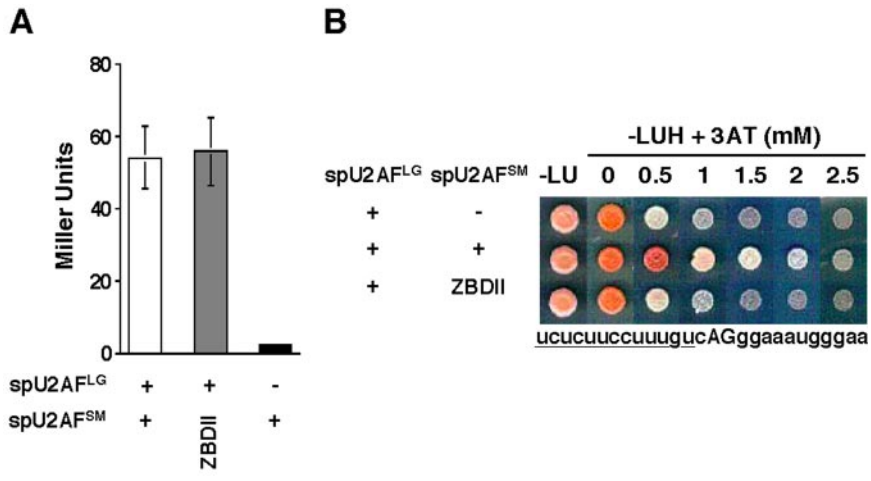

Figure 3. (A) Two-hybrid analysis of heterodimer formation in the [C157S, C163S, H167I] small subunit ZBDII mutant. Two-hybrid assays were performed as in Figure 1C. Wild-type, white bar; mutant, gray bar; negative control, black bar. (B) Plate assays to test the contribution to RNA binding of the [C157S, C163S, H167I] small subunit ZBDII mutant in the modified RNA three-hybrid system (Webb and Wise, 2004). The strength of the RNA-protein interaction is reflected by growth in the presence of increasing amounts of 3-amino-triazole (SenGupta *et al.*, 1996; Eckman *et al.*, 2002). The data shown are for the human β-globin 3′ splice site that is similar to many *S. pombe* 3′ splice sites; its sequence extending from just downstream of the branchpoint to 10 bases beyond the 3′ AG dinucleotide is shown beneath the plate assays.

notypic consequences (Figure 2) that are not shared by other fission yeast splicing factor mutants (e.g., Beales *et al.*, 2000; Urushiyama *et al.*, 1996). This proposal is counter to the model for the division of labor between the two subunits in metazoans, which is based on in vitro evidence that the large subunit participates in a subset of splicing events in the absence of a contribution from the small subunit (reviewed in Moore, 2000). Note that it remains possible that mammalian U2AF acts as a unit in vivo, since free large or small subunits are not present in significant amounts inside the cell (Zhang *et al.*, 1992). To test our functional interdependence hypothesis, we decided to perform splicing assays on chromosomally encoded RNAs extracted from two temperature-sensitive fission yeast U2AF mutants isolated in previous studies. The C387Y spU2AF^{LG} allele has been extensively characterized previously and shown to cease growth after approximately half a generation (Potashkin *et al.*, 1993; Romfo *et al.*, 1999). The [Y108A, F111A] spU2AF^{SM} allele was isolated as part of a comprehensive structure-function analysis of the small subunit (Webb and Wise, 2004), but was not analyzed with respect to its effect on growth or splicing in that study.

Shown in Figure 4A is a growth curve for the [Y108A, F111A] spU2AF^{SM} mutant, as well as an isogenic wild-type strain, at both the permissive (30°C) and nonpermissive (37°C) temperatures. The growth rate of the small subunit mutant begins to decrease ~4 h after shifting to the nonpermissive temperature and plateaus after ~10 h. To determine whether the growth defect might be due to diminished splicing, we performed RT-PCR analysis to determine the ratio of linear precursor RNA to mature mRNA for the first intron in the *ypt5* pre-mRNA (*ypt5*-I1) at three time points after the temperature shift. Even though the cells are still growing at the wild-type rate, splicing is already impaired after 2 h under nonpermissive conditions, with linear precursor representing 10% of the total *ypt5*-I1 RNA. A comparatively more dramatic accumulation of precursor (18%) is observed after 4 h, and an even higher level (21%) after 6 h. In parallel cultures grown at the permissive temperature (30°C), the fraction of precursor is very low at the 2 h time point (2%); although increases are observed in the 4- and 6-h samples (7 and 6%, respectively), the accumulation of precursor is quite modest compared with that observed at the nonpermissive temperature.

The fact that the temperature-sensitive [Y108A, F111A] fission yeast small subunit mutant does indeed display a splicing defect at the nonpermissive temperature placed us in a position to directly test our hypothesis that the two subunits of U2AF are functionally interdependent in *S. pombe*. Specifically, our model predicts that splicing of any given pre-mRNA will display 1) parallel requirements for the large and small subunits of U2AF and 2) no correlation between the strength of the signals at the 3′ splice site (branchpoint sequence/polypyrimidine tract/yAG) and the requirement for either subunit of spU2AF. Figure 5A shows splicing data for the first pre-mRNA we tested, *cdc16*-I2, at both the permissive (30°C) and nonpermissive (37°C) temperature for either the spU2AF^{SM} (left panel) or the spU2AF^{LG} (right panel) ts mutant. As an additional control, we assayed RNA from the corresponding wild-type strains at both temperatures. Because extensive data have been published for the effect of the large subunit mutant 2 h after shifting to nonpermissive conditions (Potashkin *et al.*, 1993; Romfo *et al.*, 1999) and to minimize secondary mutational effects after cessation of growth, all assays were conducted at this time point even though the *ypt5*-I1 data show that the magnitude of the small subunit splicing defect increases after longer periods of time at the nonpermissive temperature (Figure 4B). Interestingly, *cdc16*-I2 is not very efficiently spliced even at the permissive temperature or in a wild-type strain (Figure 5A). However, inactivation of spU2AF^{SM} by shifting the [Y108A, F111A] mutant to 37°C dramatically increases the level of precursor, from 24 to 60%. spU2AF^{LG}

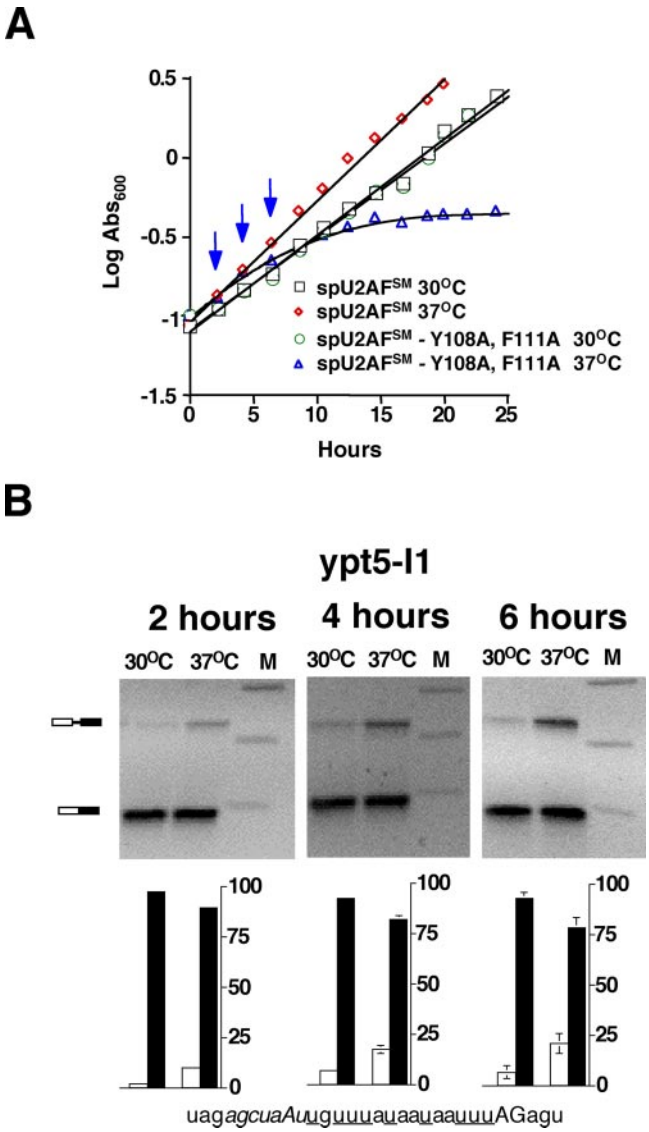

Figure 4. (A) Growth curve for the temperature-sensitive [Y108A, F111A] spU2AF^{SM} mutant. Growth of isogenic strains harboring either a wild-type or mutant allele was monitored by measuring the absorbance$_{600}$ of cultures propagated at the standard growth temperature (30°C) or at high temperature (37°C). Vertical blue arrows designate time points at which RNA was extracted. (B) RT-PCR assays of splicing in the ts spU2AF^{SM} mutant. (Top) Gel electrophoretic analysis of products from chromosomally expressed *ypt5*-I1 at three different time points after the shift to nonpermissive temperature and in parallel cultures propagated at the permissive temperature. The positions of linear pre-mRNA and mature mRNA are indicated schematically at the left. Bottom: histogram showing quantitation of RT-PCR data. White bars, percent precursor mRNA; black bars, percent mature mRNA. Error bars, SD for three RT-PCR splicing assays. Shown at the bottom is the sequence of the 3′ end of *ypt5*-I1 with the branchpoint sequence indicated in italics, the pyrimidine tract underlined, and the terminal AG in uppercase.

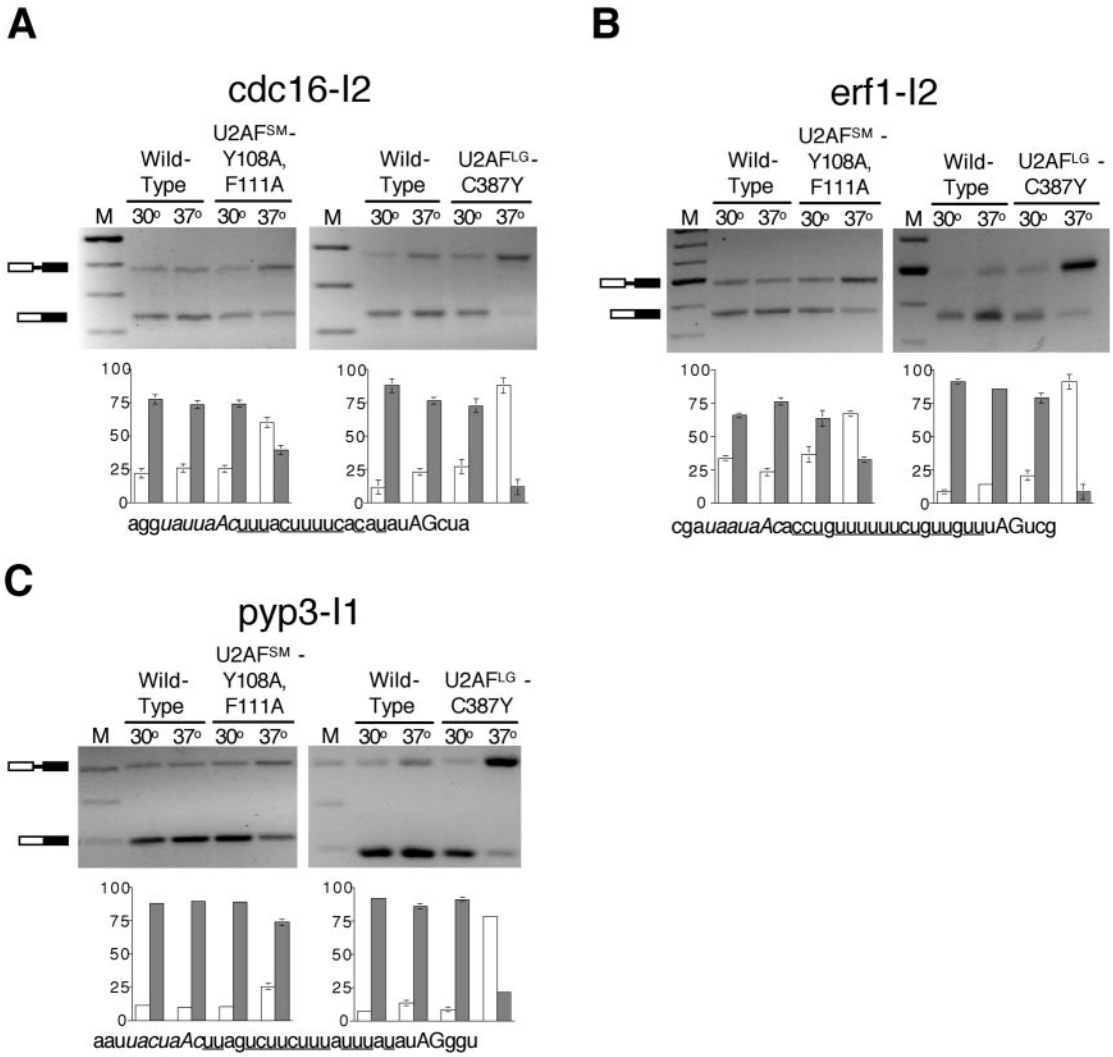

Figure 5. RT-PCR assays of *cdc16*-I2, *erf1*-I2, and *pyp3*-I1 splicing in the ts spU2AF^{SM} and spU2AF^{LG} mutants. (A) Top left: gel electrophoretic analysis of products from *cdc16*-I2 in the spU2AF^{SM} [Y108A, F111A] mutant. Bottom left: histogram showing quantitation of RT-PCR data with percent precursor mRNA indicated by white bars and percent mature mRNA indicated by black bars. Error bars, SD for three RT-PCR splicing assays. (Right: as in the left panels except that the experiment was performed with the spU2AF^{LG} C387Y mutant. Bottom: the sequence of the 3′ end of *cdc16*-I2 with the branchpoint sequence indicated in italics, the pyrimidine tract underlined, and the terminal AG in uppercase. (B) As in A except that the splicing data are for *erf1*-I2. (C) As in A except that the splicing data are for *pyp3*-I1.

inactivation causes an even more dramatic splicing defect, with <10% mature mRNA remaining after 2 h at the nonpermissive temperature. Splicing of this intron was similarly impaired when we used a different means of reducing the levels of either U2AF subunit, namely metabolic depletion (Webb and Wise, 2004).

Our finding that *cdc16*-I2 precursor accumulates in the absence of functional *S. pombe* U2AF small subunit is notable in light of the model for metazoan U2AF function, which postulates that introns containing strong polypyrimidine tracts do not require the small subunit for splicing (reviewed in Moore, 2000). The polypyrimidine tract of *cdc16*-I2 consists of 11 pyrimidines with 3 single purine interruptions (Figure 5A, bottom panel), which places it at the "strong" end of *S. pombe* polypyrimidine tracts (Zhang and Marr, 1994; Wood *et al.*, 2002). To determine whether fission yeast pre-mRNAs with extensive polypyrimidine tracts generally have a strong dependence on both subunits of U2AF, we examined the splicing profile of *erf1*-I2, which has a branchpoint to 3′ splice site distance and base composition comparable to *cdc16*-I2 (Figure 5B). Shifting the spU2AF^{SM} mutant to 37°C yields substantially more precursor (67%) than at 30°C (36%), demonstrating that this intron also requires the small subunit for efficient splicing. As for *cdc16*-I2, inactivation of spU2AF^{LG} results in a higher level of unspliced *erf1*-I2 (>90%; Figure 5B).

Because *erf1* and *cdc16* are multi-intronic, we examined the splicing profile of *pyp3*, a pre-mRNA interrupted by a single central intron with above average 3′ pyrimidine content for *S. pombe*. *pyp3*-I1 reproducibly shows modest but readily discernible precursor accumulation in the spU2AF^{SM} mutant at 37°C (25%) and a more dramatic splicing defect in the spU2AF^{LG} mutant (76%; Figure 5C). We conclude that, in *S. pombe*, the small subunit of U2AF is required for splicing of pre-mRNAs with strong polypyrimidine tracts, supporting our hypothesis that when one subunit of U2AF is

required for splicing of a given pre-mRNA in *S. pombe*, so is the other.

Splicing Assays on a Panel of Introns Reveal Diverse but Generally Parallel Requirements for the Two Subunits of S. pombe *U2AF*

In an effort to identify introns that show distinct requirements for spU2AF^{LG} and spU2AF^{SM}, we analyzed nineteen additional introns that span the continuum of branchpoint to 3′ splice site distances in this organism. Note that branchpoint assignments are based on in silico sequence comparisons, as physical mapping has been impeded by the finding that many splice site mutants that lead to lariat accumulation in mammals and budding yeast block the first step of splicing in fission yeast (Romfo and Wise, 1997; Alvarez and Wise, 2001). Nevertheless, we believe these assignments are likely to be accurate because branchpoint sequences are much more readily recognized in *S. pombe* than in metazoans, although less so than in *S. cerevisiae* (Wood *et al.*, 2002). Although the first two positions of the UACUAAC consensus that is virtually invariant in budding yeast are not appreciably conserved in fission yeast, the other five positions show substantial conservation, particularly when purine/purine and pyrimidine/pyrimidine substitutions are taken into account. The frequency breakdown among the 4565 total introns is as follows: ctaac (1943), ctaat (1038), ttaac (714), ctgac (238), ttaat (178), cttac (130), ctaaa (104), ttgac (60), ctgat (60), ataac (50), ttgat (36) and gtaac (14); taken from http://www.sanger.ac.uk/Projects/S_pombe/intron.shtml.

The entire panel of introns examined, shown schematically in Figure 6A, includes the two introns identified by the *S. pombe* genome project with the longest (SPCC16A11.08-I2) and shortest (*swi4*-I1) known distances between the designated branchpoint sequence and the terminal 3′ YAG. The other 17 introns were selected to represent a continuum of branchpoint to 3′ splice site distances and variable pyrimidine contents in this interval. Quantitation of the splicing assays is depicted in Figure 6B; for simplicity, the isogenic wild-type controls are unpublished data, but these strains did not display a significant change in precursor accumulation at 37°C compared with 30°C (≤13%). The first notable result is that *chk1*-I3, which contains just three nucleotides, only one of them a pyrimidine, between the branchpoint sequence and 3′ splice site (Figure 6A, 20), displays a strong requirement for both subunits of *S. pombe* U2AF (Figure 6B, 20). The 3′ architecture of *erf1*-I3 is similar to *chk1*-I3, and this intron displays similar levels of precursor accumulation in the spU2AF mutants (Figure 6B, 21). *swi4*-I1, which has an even shorter branchpoint to 3′ splice site distance, is affected to a lesser extent by mutational inactivation of either subunit of spU2AF (Figure 6B, 22). Finally, three of the introns with short branchpoint to 3′ splice site distances (Figure 6B, 17–19) exhibit moderate precursor accumulation upon inactivation of spU2AF^{LG} and no discernible splicing defect in the spU2AF^{SM} mutant.

The mean branchpoint to 3′ splice site distance is 9.7 nucleotides in *S. pombe* (Zhang and Marr, 1994), and introns close to this average also show diverse U2AF requirements for efficient splicing (Figure 6B, 9–13) that do not correlate in any obvious way with 3′ pyrimidine content. More noteworthy is the fact that the intron with the longest branchpoint to 3′ splice site distance in the *S. pombe* genome does not exhibit dramatic accumulation of precursor after mutational inactivation of either the small or the large subunit of U2AF (Figure 6B, 1). The branchpoint to 3′ splice site interval of SPCC16A11.08-I2 is biased toward pyrimidines (24/42 nucleotides), and a similar ratio (19/40 nucleotides) is found in SPCC830.12-I1 (Figure 6A, 2), which also has an unusually long 3′ interval. Splicing of the latter intron is affected to a modest degree by inactivation of the spU2AF large subunit and less so by inactivation of the small subunit (Figure 6B, 2).

Assaying splicing of different introns in multi-intronic pre-mRNAs after U2AF inactivation demonstrates that the order in which an intron appears is not a key determinant of U2AF dependence in *S. pombe*. For example, the second and third (middle) introns and the fourth (terminal) intron of *erf1* all show a pronounced requirement for both subunits of the *S. pombe* heterodimer (Figure 6B, 5, 21, and 11). In contrast, introns 1, 2, and 3 of *cdc16* exhibit variable spU2AF requirements, with the first intron remaining largely unspliced after inactivation of either spU2AF^{LG} or spU2AF^{SM} (Figure 6B, 13). *cdc16*-I3 accumulates precursor only after inactivation of the large subunit (Figure 6B, 19), and *cdc16*-I1 does not accumulate precursor after inactivation of either subunit of spU2AF (Figure 6B, 13). The observation that individual introns within the same pre-mRNA are retained to varying extents after spU2AF inactivation strongly argues against the idea that differences in RNA stability due to either nuclear turnover or cytoplasmic nonsense-mediated decay account for the distinct levels of precursor observed in different pre-mRNAs.

U2AF-dependence Does Not Correlate with Other Obvious Features of S. pombe *pre-mRNAs*

In an effort to determine the mechanistic basis for the differential U2AF requirements in *S. pombe*, we proceeded to examine features of the 22 pre-mRNAs in addition to 3′ pyrimidine content, branchpoint to 3′ splice site distance and intron position within multi-intronic precursors. First, because hsU2AF^{LG} binds to and collaborates with SF1/BBP (Berglund *et al.*, 1998; Selenko *et al.*, 2003), we first asked whether the strength of the branchpoint correlates, either directly or inversely, with spU2AF-dependence; no relation was found between the match to the branchpoint consensus (Zhang and Marr, 1994) and spU2AF requirements (see Figure 6). Second, given that introns are bridged by a complex anchored at one end by the U1 snRNP and at the other by U2AF (Abovich *et al.*, 1994; Berglund *et al.*, 1998), we examined the 5′ splice sites of the 22 introns; there was also no correlation between the strength of the 5′ splice site and spU2AF requirements (see Figure 6). Finally, because U2AF can be recruited to weak 3′ splice sites by exonic enhancers (Zuo and Maniatis, 1996) that promote splicing in *S. pombe* (Webb, Romfo, and Wise, unpublished data), we looked for a correlation with the presence of purine-rich elements downstream; again, none was found (unpublished data). We conclude that neither known *cis*-acting splicing signals nor other obvious architectural features dictate the requirement for U2AF during splicing in *S. pombe*. Similarly, the Ares laboratory found that models for features recognized by *S. cerevisiae* splicing factors did not hold up when a more extensive panel of pre-mRNAs was examined (Clark *et al.*, 2002).

Although we cannot definitively ascertain which features of the pre-mRNA determine spU2AF requirements, the data presented here reinforce the view that the polypyrimidine tract plays a diminished role in *S. pombe* splicing compared with metazoans. This is consistent with the observation that two different *S. pombe* introns could not be converted to AG-independence by expansion of the polypyrimidine tract (Romfo and Wise, 1997), in contrast to AG-dependent mammalian substrates (Reed, 1989). Thus, the information content of the polypyrimidine tract alone is not sufficient for 3′

A

#	Gene Name	5′ Splice Site	Branchpoint Sequence	Polypyrimidine Tract	3′ Splice Site
1	SPCC16A11.08-I2	GUAAGU	*UAUUAAC*	AUGGGCUGUGUGCAAUUCAUUGUACACACAUGCUCCGCUGUUUAG	UAA
2	SPCC830.12-I1	GUAUGA	*UGCUAAC*	--CAAUUAUCCAUCACAUGAGAGCAUGUGUUGGUCUUAAAUUUAG	GCU
3	SPAC17A5.16-I3	GUAUGA	*UACUAAU*	----------GUAUUCGUUUUUAUGUUUAUUAG	CUU
4	pyp3-I1	GUUAGG	*UACUAAC*	----------UUAGUCUUCUUUAUUUAUAUAG	GGU
5	erf1-I2	GUAUGA	*UAAUAAC*	----------ACCUGUUUUUUCUGUUGUUUAG	UCG
6	mcs2-I2	GUAUGU	*AGCUAAC*	----------CAUUGUUUUUCUUACAUUAG	GUU
7	cdc16-I2	GUAAGU	*UAUUAAC*	----------UUUACUUUUCACAUAUAG	CUA
8	ypt5-I1	GUAGGU	*AGCUAAU*	----------UGUUUAUAAUAAUUUAG	AGU
9	cdc17-I2	GUAUGA	*UACUAAC*	----------GUCUUUUUUUACAUUAG	UUG
10	SPAC22F8.13-I2	GUAAGU	*UACUGAU*	----------GUGUGCGUUUGUAG	AAU
11	erf1-I4	GUAAAU	*UACUGAU*	----------CAAUUUUUUAG	GGC
12	cdc2-I2	GUAAGU	*UUCUAAC*	----------CCUUUUUUAAG	ACU
13	cdc16-I1	GUAAGU	*UACUAAC*	----------UCAAUUACAG	UUA
14	pim1-I1	GUAAGU	*UGCUAAC*	----------AUACUAG	UGU
15	rad9-I3	GUAUGU	*CAUUAAC*	----------UUUAUAG	CAA
16	pck1-I1	GUAGUA	*UAUUAAC*	----------CCCAUAG	AUU
17	rad26-I2	GUAAGU	*UUCUAAC*	----------AAAUUAG	AAU
18	top1-I2	GUAUGU	*GACUAAU*	----------UGUUUAG	AAU
19	cdc16-I3	GUAAGU	*UGCUAAC*	----------GAUAAAG	CCC
20	chk1-I3	GUAAGU	*AACUAAU*	----------GAUCAG	CGA
21	erf1-I3	GUAAAU	*UACUGAC*	----------UUGCAG	GUC
22	swi4-I1	GUAAGU	*UUCUUAC*	----------AGUAG	CCU

B

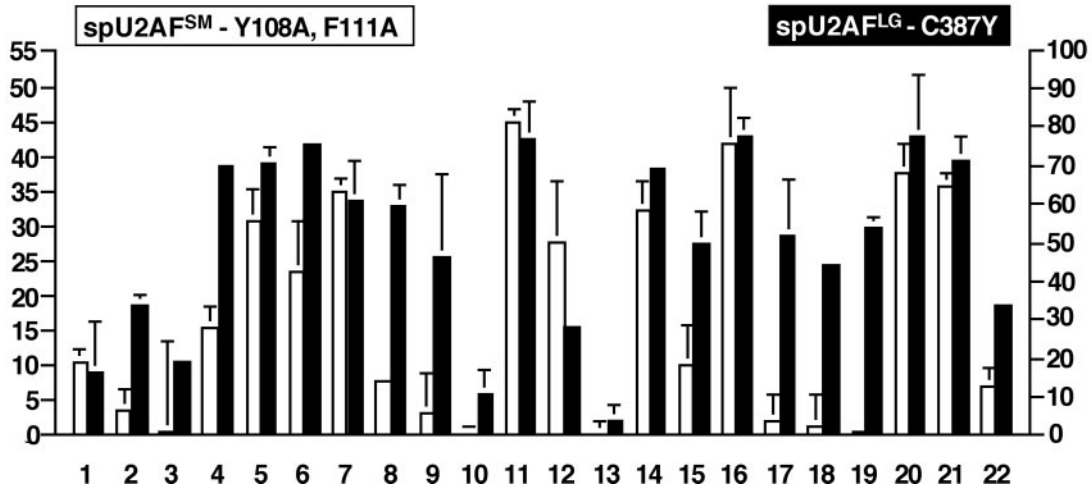

Figure 6. Analysis of splicing in vivo for 22 introns in the ts spU2AF^{SM} and spU2AF^{LG} mutants. (A) Each number is followed by the gene name and sequence of the 5′ splice site, branchpoint, polypyrimidine tract, 3′ splice site, and three nucleotides beyond the AG at the intron/exon boundary. Complete sequences can be found at http://www/Sanger.ac.uk/Projects/S_pombe/. (B) Histograms showing quantitation of RT-PCR assays for the 22 introns depicted in A after heat inactivation of either subunit. Data were collected as in Figure 5 but are expressed as the percent precursor observed at 30°C subtracted from the percent precursor observed at 37°C (Δ precursor accumulation from 30 to 37°C). White bars, data for the spU2AF^{SM} [Y108A, F111A] mutant; black bars, the spU2AF^{LG} C387Y mutant data. Note that the scales are different for each subunit, owing to the more dramatic splicing defects caused by the large subunit ts allele at the 2 h time point (see text for details).

splice site recruitment in *S. pombe*. Stated otherwise, spU2AF^{SM} recognition of the 3′ splice site cannot be bypassed by improving the target sequence for spU2AF^{LG}. In aggregate, our results can be explained most parsimoniously by a model in which the small and large subunits of U2AF collaborate during initial 3′ splice site recognition in *S. pombe*. Fifteen of the 22 introns analyzed in this report display parallel spU2AF subunit requirements for efficient splicing. Thirteen of these exhibit readily discernible splicing defects after inactivation of either subunit of the spU2AF heterodimer, and two do not. Most notably, nine of the 10 introns whose splicing is most dramatically affected by

spU2AF^{SM} inactivation are among the 10 most strongly affected by spU2AF^{LG} inactivation (Figure 6B, 4–8, 11, 14, 16, 20, and 21). The more dramatic splicing defects observed with the large subunit mutant suggest that it is a more stringent ts allele, consistent with the Rio laboratory's recent finding that a mutation equivalent to spU2AF^{LG} C387Y conferred a temperature-sensitive phenotype in *Drosophila*, whereas other point mutations that yielded ts phenotypes in fission yeast did not (Blanchette *et al.*, 2004). This interpretation is also consistent with our finding that the small subunit mutant displays more dramatic growth and splicing defects later in the time course (Figure 4), suggesting that it may be impaired in folding or assembly into the heterodimer, whereas the rapid inactivation of the large subunit has been interpreted as evidence of a functional defect (Potashkin *et al.*, 1993; Romfo *et al.*, 1999).

DISCUSSION

In this study, we first demonstrated by ablation analysis that each of the five domains of the *S. pombe* U2AF large subunit is independently essential for viability. Second, we isolated spU2AF large and small subunit mutants that share a remarkably similar and highly unusual phenotype; in conjunction with the dominant negative effects of large subunit mutants that lack the RS domain but can still bind the small subunit, this observation led us to hypothesize an extraordinary degree of cooperation between the heterodimeric partners in fission yeast. To test this idea, we examined the splicing in vivo of a diverse panel of pre-mRNAs after inactivation of either spU2AF^{LG} or spU2AF^{SM}. In aggregate, the results of this study provide strong evidence from diverse experimental strategies to support the view that the two subunits of *S. pombe* U2AF function in a highly collaborative manner in vivo.

Novel Contributions from Genetics Shed Light on U2AF Function

Although the present study reports the first comprehensive domain ablation analysis of the U2AF large subunit in vivo, reverse genetic experiments have previously been conducted on the two N-terminal domains in *Drosophila*. As noted in *Results*, our finding that a partial deletion of the spU2AF^{LG} linker region implicated in small subunit interactions confers a growth defect echoes the reduced viability observed in flies carrying alleles with multiple point mutations in the linker as their sole source of the large subunit (Rudner *et al.*, 1998c). On the other hand, the results of deleting the U2AF^{LG} RS domain differ between flies and fission yeast. In contrast to the dominant lethality observed in fission yeast, simple deletion of the RS domain of dmU2AF^{LG} was phenotypically silent (Rudner *et al.*, 1998b). However, when this allele was combined with a deletion of the C-terminal RS/G-rich domain of dmU2AF^{SM}, lethality ensued. The authors concluded that the RS domains of the two subunits of U2AF have redundant or overlapping functions in *Drosophila*. Notably, fission yeast is the only organism in which only one of the U2AF subunits contains a domain with repetitive amino acid sequences (Zorio and Blumenthal, 1999a). Thus, the inability of the *S. pombe* large subunit to function without its RS domain may simply reflect the absence of a repeat-containing domain at the *S. pombe* U2AF^{SM} C-terminus. In other words, it is likely that evolution has carried out a successful experiment in fission yeast similar to the domain deletion analysis carried out by Rio and colleagues in the fruit fly.

Mutations designed to abolish the capacity of the two canonical RRMs to bind RNA have not been studied previously in vivo. Notably, both the [F247D, I249D] substitution in RRM1 and the [F353D, F355D] RRM2 mutant produce recessive lethality, in contrast to the dominant effect of deleting the N-terminal RS domain. In light of evidence that the N-terminal domain of human U2AF^{LG} promotes the transition from the E (early) complex containing U1 snRNP, U2AF, and SF1/BBP to the A complex (prespliceosome) by facilitating annealing of U2 snRNA to the branchpoint sequence (Valcarcel *et al.*, 1996), a reasonable interpretation of our data is that the protein lacking an RS domain forms E complex but is unable to continue spliceosome assembly, whereas a mutant unable to bind RNA does not even enter the pathway. The relief of dominance when the linker region is also eliminated (Romfo *et al.*, 1999) suggests further that U2AF heterodimer formation is also necessary to form E complex, consistent with our splicing data supporting parallel requirements for the two subunits in vivo. It is these functional data that distinguish our study from those carried out previously, as splicing was not analyzed in the *Drosophila* linker domain mutants (Rudner *et al.*, 1998c), and introns with dramatic splicing defects (i.e., that showed more than a few percent precursor accumulation) were not identified in the fly U2AF^{LG} temperature-sensitive mutants (Blanchette *et al.*, 2004) even though one of these is analogous to the allele we analyzed here (C387Y). One possible reason for the discrepancy is that nuclear RNA turnover is much more rapid or efficient in *Drosophila* than in *S. pombe*. Most importantly, our study was the first to analyze both subunits of U2AF and was uniquely possible in *S. pombe*, the only organism in which a conditional small subunit mutant has been identified.

A key question is whether the few introns that showed no or barely detectable splicing defects even in the very tight fission yeast large subunit conditional mutant are truly spU2AF-independent. We have previously reported that different introns display differential splicing defects in the presence of spU2AF large subunit mutations (Romfo *et al.*, 1999). One possible explanation for why some introns show little response to spU2AF mutations even at the nonpermissive temperature is that they have better spU2AF-binding sites capable of attracting the limiting quantities of functional spU2AF. However, given the lack of a correlation between spU2AF dependence and 3′ pyrimidine content, or for that matter any other obvious feature of the intron or downstream exon, we favor the alternative explanation that these data reflect the cooperative nature of spliceosome assembly in vivo.

The idea that U2AF's role in some splicing events in vivo can be masked by redundant interactions with other factors may be related to another apparent discrepancy between our work and results generated in vitro. In particular, structural and biochemical data support the view that a tryptophan corresponding to position 135 of *S. pombe* U2AF^{LG} is crucial for heterodimer formation (Kielkopf *et al.*, 2001), whereas our data demonstrate that this amino acid can be mutated to a phenylalanine in vivo with no discernible phenotypic consequences. Trp135 is found in the linker region of the large subunit and we have shown previously that mutating the corresponding tryptophan (W128) in the ΨRRM of U2AF^{SM} to either phenylalanine or alanine is tolerated in fission yeast (Webb and Wise, 2004). Thus, experiments carried out in vitro with only two components may amplify the importance of particular interactions.

Is U2AF Function in S. pombe *Unique?*

Recent biochemical data demonstrate that, in *S. pombe*, the U2AF heterodimer exists in a tight 1:1:1 complex with SF1 (Huang *et al.*, 2002). The authors of this study proposed that *S. pombe* has optimized recognition of the 3′ splice site via the concerted interaction of the SF1/spU2AF^{LG}/spU2AF^{SM} complex and the tripartite intronic 3′ splicing signals. The parallel splicing defects we observe after separate inactivation of the large or small subunit of spU2AF are consistent with participation of this factor in such a streamlined system of 3′ splice site recognition. A related model for concerted 3′ splice site recognition by the U2AF heterodimer has been proposed for *C. elegans*, where the intron/exon boundary is preceded by a short, highly conserved polypyrimidine tract followed immediately by the universal AG dinucleotide (U_4CAG/R), and the branchpoint sequence has diverged to an unrecognizable state (Blumenthal and Steward, 1997; Zorio and Blumenthal, 1999b).

It remains to be determined whether an SF1/hsU2AF^{LG}/hsU2AF^{SM} complex exists in mammalian cells or if such a complex concurrently recognizes the branchpoint/polypyrimidine tract/AG dinucleotide at the 3′ splice site. In support of this possibility, an interaction between the large subunit of human U2AF and SF1 promotes cooperative binding to an RNA containing a branchpoint and polypyrimidine tract in vitro (Berglund *et al.*, 1998). Concerted recognition is an attractive model to explain how bona fide 3′ splice sites are correctly identified in mammals, where reasonable matches to the branchpoint and 3′ splice site consensus including the polypyrimidine tract occur randomly every 24 and 490 nucleotides, respectively (Burge *et al.*, 1999). Clearly, however, splicing of a subset of metazoan introns does not require the small subunit of U2AF, at least in vitro, and thus the *S. pombe* model may not apply to such pre-mRNAs. A dichotomy between fission yeast and mammals is supported by the observation that phosphorylation of a serine that is conserved among SF1 orthologues in metazoans, but not in *S. pombe* (Mazroui *et al.*, 1999), prevents binding to the large subunit of hsU2AF (Wang *et al.*, 1999). If the available hsU2AF and SF1 are not obligatorily bound together in a complex but rather are free to dissociate in a phosphorylation-dependent manner, this could provide an opportunity for these factors to participate in temporal and spatial regulation of splicing that is not possible in *S. pombe*. Indeed, inhibition of *Drosophila msl-2* splicing by Sex-lethal appears to rely on an unusually long branchpoint to 3′ splice site distance to allow the alternative splicing factor to displace U2AF (Merendino *et al.*, 1999). In addition, the presence in metazoans of genes related to the hsU2AF small subunit (Tronchere *et al.*, 1997; Mount and Salz, 2000; Tupler *et al.*, 2001; Pacheo *et al.*, 2004) as well as tissue-specific alternatively spliced isoforms (Pacheo *et al.*, 2004) suggests the possibility of modular hsU2AF function, wherein 3′ splice site recognition depends on the attributes of different heterodimeric partners for hsU2AF^{LG}.

Collectively, the data from a variety of studies in metazoans and both budding and fission yeast suggest that, unlike the evolutionarily conserved process of 5′ splice site recruitment via complementary base-pairing to U1 snRNA, the interplay between *cis*-acting elements and *trans*-acting factors during initial recognition of the 3′ splice site has diverged significantly during evolution.

ACKNOWLEDGMENTS

We thank Frank Campbell, Jonatha Gott, Michael Harris, Hua Lou, David McPheeters, and Helen Salz for critical comments on the manuscript. We thank Carissa Romano for expert technical assistance, the curators of the Sanger Center *S. pombe* genome project for providing a list of introns classified according to branchpoint to 3′ splice site distance and pyrimidine content, and Shelley Sazer (Baylor College of Medicine) for prep41X-imp2. This research was supported by a grant to J.A.W. from the National Institutes of Health; C.J.W. was supported in part through a Cell and Molecular Biology Training Grant awarded through the National Institute of General Medical Sciences.

REFERENCES

Abovich, N., Liao, X., and Rosbash, M. (1994). The yeast MUD2 protein: an interaction with PRP11 defines a bridge between commitment complex and U2 snRNP addition. Genes Dev. *8*, 843–854.

Alvarez, C. J., Romfo, C. M., VanHoy, R. W., Porter, G. L., and Wise, J. A. (1996). Mutational analysis of U1 function in *Schizosaccharomyces pombe*: pre-mRNAs differ in the extent and nature of their requirements for this snRNA *in vivo*. RNA *2*, 404–418.

Alvarez, C. J., and Wise, J. A. (2001). Activation of a cryptic 6′ splice site by U1 snRNA. RNA *7*, 342–350.

Banerjee, H., Rahn, A., Gawande, B., Guth, S., Valcarcel, J., and Singh, R. (2004). The conserved RNA recognition motif 3 of U2 snRNA auxiliary factor (U2AF 65) is essential *in vivo* but dispensable for activity *in vitro*. RNA *10*, 240–253.

Beales, M., Flay, N., McKinney, R., Habara, Y., Ohshima, Y., Tani, T., and Potashkin, J. (2000). Mutations in the large subunit of U2AF disrupt pre-mRNA splicing, cell cycle progression and nuclear structure. Yeast *16*, 1001–1013.

Berglund, J. A., Abovich, N., and Rosbash, M. (1998). The splicing factor BBP interacts specifically with the pre-mRNA branchpoint sequence UACUAAC. Genes Dev. *12*, 858–867.

Blanchette, M., Labourier, E., Green, R. E., Brenner, S. E., and Rio, D. C. (2004). Genome-wide analysis reveals an unexpected function for the *Drosophila* splicing factor U2AF^{50} in the nuclear export of intronless mRNAs. Mol. Cell *14*, 775–786.

Blumenthal, T., and Steward, K. (1997). RNA processing and gene structure. In: C. elegans II, ed. D. Riddle, T. Blumenthal, B. Meyers, and J. Priess, Cold Spring Harbor, NY: Cold Spring Harbor Laboratory Press, 117–145.

Burge, C. B., Tuschl, T., and Sharp, P. A. (1999). Splicing of Precursors to mRNAs by the Spliceosome. In: The RNA World, ed. R. Gesteland, T. Cech, and J. Atkins, Cold Spring Harbor, NY: Cold Spring Harbor Laboratory Press, 525–560.

Caceres, J. F., and Krainer, A. R. (1993). Functional analysis of pre-mRNA splicing factor SF2/ASF structural domains. EMBO J. *12*, 4715–4726.

Clark, T. A., Sugnet, C. W., and Ares, M., Jr. (2002). Genomewide analysis of mRNA processing in yeast using splicing-specific microarrays. Science *296*, 907–910.

Davies, R. C., Calvio, C., Bratt, E., Larsson, S. H., Lamond, A. I., and Hastie, N. D. (1998). WT1 interacts with the splicing factor U2AF65 in an isoform-dependent manner and can be incorporated into spliceosomes. Genes Dev. *12*, 3217–3225.

Eckmann, C. R., Kraemer, B., Wickens, M., and Kimble, J. (2002). GLD-3, a bicaudal-C homolog that inhibits FBF to control germline sex determination in *C. elegans*. Dev. Cell *3*, 697–710.

Fewell, S. W., and Woolford, J. R. (1999). Ribosomal protein S14 of *Saccharomyces cerevisiae* regulates its expression by binding to RPS14B pre-mRNA and to 18S rRNA. Mol. Cell. Biol. *19*, 826–834.

Fleckner, J., Zhang, M., Valcarcel, J., and Green, M. R. (1997). U2AF^{65} recruits a novel human DEAD box protein required for the U2 snRNP-branchpoint interaction. Genes Dev. *11*, 1864–1872.

Gozani, O., Potashkin, J., and Reed, R. (1998). A potential role for U2AF-SAP 155 interactions in recruiting U2 snRNP to the branch site. Mol. Cell. Biol. *18*, 4752–4760.

Guth, S., Tange, T. O., Kellenberger, E., and Valcarcel, J. (2001). Dual function for U2AF^{35} in AG-dependent pre-mRNA splicing. Mol. Cell. Biol. *21*, 7673–7681.

Huang, T., Vilardell, J., and Query, C. (2002). Pre-spliceosomal formation in *S. pombe* requires a stable complex of SF1–U2AF59–U2AF23. EMBO J. *21*, 5516–5526.

Ito, T., Muto, Y., Green, M. R., and Yokoyama, S. (1999). Solution structures of the first and second RNA-binding domains of human U2 small nuclear ribonucleoprotein particle auxiliary factor (U2AF^{65}). EMBO J. *18*, 453–4534.

James, P., Halladay, J., and Craig, E. A. (1996). Genomic libraries and a host strain designed for highly efficient two-hybrid selection in yeast. Genetics *144*, 1425–1436.

Kanaar, R., Roche, S. E., Beall, E. L., Green, M. R., and Rio, D. C. (1993). The conserved pre-mRNA splicing factor U2AF from *Drosophila*: requirement for viability. Science *262*, 569–573.

Kielkopf, C. L., Rodionova, N. A., Green, M. R., and Burley, S. K. (2001). A novel peptide recognition mode revealed by the X-ray structure of a core $U2AF^{35}/U2AF^{65}$ heterodimer. Cell *106*, 595–605.

Kielkopf, C. L., Lucke, S., and Green, M. R. (2004). U2AF homology motifs: protein recognition in the RRM world. Genes Dev. *18*, 1513–1526.

Le Goff, X., Utzig, S., and Simanis, V. (1999). Controlling septation in fission yeast: finding the middle, and timing it right. Curr. Genet. *35*, 571–584.

Mazroui, R., Puoti, A., and Kramer, A. (1999). Splicing factor SF1 from *Drosophila* and *Caenorhabditis*: presence of an N-terminal RS domain and requirement for viability. RNA *5*, 1615–1631.

Merendino, L., Guth, S., Bilboa, D., Martinez, C., and Valcarcel, J. (1999). Inhibition of msl-2 splicing by Sex-lethal reveals interaction between $U2AF^{35}$ and the 3′ splice site AG. Nature *402*, 838–841.

Moore, M. (2000). Intron recognition comes of AGe. Nature *7*, 14–16.

Mount, S. M., and Salz, H. K. (2000). Pre-messenger RNA processing factors in the *Drosophila* genome. J. Cell Biol. *150*, F37–F44.

Pacheo, T. R., Gomes, A. Q., Barbosa-Morais, N. L., Benes, V., Ansorge, W., Wollerton, M., Smith, C. W., Valcarcel, J., and Carmo-Fonseca, M. (2004). Diversity of vertebrate splicing factor $U2AF^{35}$: identification of alternatively spliced U2AF1 mRNAs. J. Biol. Chem. *279*, 27039–27049.

Page-McCaw, P., Amonlirdviman, K., and Sharp, P. (1999). PUF60, a novel $U2AF^{65}$-related splicing activity. RNA *5*, 1548–1560.

Potashkin, J., Naik, K., and Wentz-Hunter, K. (1993). U2AF homolog required for splicing *in vivo.* Science *262*, 573–575.

Reed, R. (1989). The organization of 3′ splice-site sequences in mammalin introns. Genes Dev. *3*, 2113–2123.

Romfo, C., Lakhe-Reddy, S., and Wise, J. A. (1999). Molecular genetic analysis of $U2AF^{59}$ in *Schizosaccharomyces pombe*: differential sensitivity of introns to mutational inactivation. RNA *5*, 49–65.

Romfo, C. M., and Wise, J. A. (1997). Both the polypyrimidine tract and the 3′ splice site function prior to the first step of splicing in fission yeast. Nucleic Acids Res. *25*, 4658–4665.

Rudner, D., Breger, K., Kanaar, R., Adams, M., and Rio, D. (1998a). RNA binding activity of heterodimeric splicing factor U2AF: at least one RS domain is required for high-affinity binding. Mol. Cell. Biol. *18*, 4004–4011.

Rudner, D. Z., Breger, K. S., and Rio, D. (1998b). Molecular genetic analysis of the heterodimeric splicing factor U2AF: the RS domain on either the large or small *Drosophila* subunit is dispensable *in vivo.* Genes Dev. *12*, 1010–1021.

Rudner, D., Kanaar, R., Breger, K., and Rio, D. (1998c). Interaction between subunits of heterodimeric splicing factor U2AF is essential *in vivo.* Mol. Cell. Biol. *18*, 1765–1773.

Rudner, D., Kanaar, K., Breger, S., and Rio, D. (1996). Mutations in the small subunit of the *Drosophila* U2AF splicing factor cause lethality and developmental defects. Proc. Natl. Acad. Sci. USA *93*, 10333–10337.

Ruskin, B., Zamore, P. D., and Green, M. R. (1988). A factor, U2AF, is required for U2 snRNP binding and splicing complex assembly. Cell *52*, 207–219.

Selenko, P., Gregorovic, G., Sprangers, R., Stier, G., Rhani, Z., Kramer, A., and Sattler, M. (2003). Structural basis for the molecular recognition between human splicing factors U2AF65 and SF1/mBBP. Mol. Cell *11*, 965–976.

SenGupta, D. J., Zhang, B., Kraemer, B., Pochart, P. Fields, S., and Wickens, M. (1996). A three-hybrid system to detect RNA-protein interactions *in vivo.* Proc. Natl. Acad. Sci. USA *93*, 8496–8501.

Singh, R., Valcarcel, J., and Green, M. R. (1995). Distinct binding specificities and functions of higher eukaryotic polypyrimidine tract-binding proteins. Science *268*, 1173–1176.

Tronchere, H., Wang, X., and Fu, X. D. (1997). A protein related to $U2AF^{35}$ that interacts with U2AF65 and SR proteins in splicing of pre-mRNA. Nature *388*, 397–400.

Tupler, R., Perini, G., and Green, M.R. (2001). Expressing the human genome. Nature *409*, 832–833.

Uruyishiyama, S., Tani, T., and Ohshima, Y. (1996). Isolation of novel pre-mRNA splicing mutants of *Schizosaccharomyces pombe.* Mol. Gen. Genet. *253*, 118–127.

Vagner, S., Vagner, C., and Mattaj, I. W. (2000). The carboxyl terminus of vertebrate poly(A) polymerase interacts with $U2AF^{65}$ to couple 3′-end processing and splicing. Genes Dev. *14*, 403–413.

Valcarcel, J., Gaur, R. K., Singh, R., and Green, M. R. (1996). Interaction of $U2AF^{65}$ RS region with pre-mRNA branch point and promotion of base pairing with U2 snRNA. Science *273*, 1706–1709.

Wang, X., Bruderer, S., Rafi, Z., Xue, J., Milburn, P. J., Kramer, A., and Robinson, P. J. (1999). Phosphorylation of splicing factor SF1 on Ser20 by cGMP-dependent protein kinase regulates spliceosome assembly. EMBO J. *18*, 4549–4559.

Webb, C. J., and Wise, J. A. (2004). The splicing factor U2AF small subunit is functionally conserved between fission yeast and humans. Mol. Cell. Biol. *24*, 4229–4240.

Wentz-Hunter, K., and Potashkin, J. (1996). The small subunit of the splicing factor U2AF is conserved in fission yeast. Nucleic Acids Res. *24*, 1849–1854.

Wood, V. *et al.* (2002). The genome sequence of *Schizosaccharomyces pombe.* Nature *415*, 871–880.

Wu, S., Romfo, C., Nilsen, T., and Green, M. (1999). Functional recognition of the 3′ splice site AG by the splicing factor $U2AF^{35}$. Nature *402*, 832–835.

Zamore, P. D., and Green, M. R. (1991). Biochemical characterization of U2 snRNP auxiliary factor: an essential pre-mRNA splicing factor with a novel intranuclear distribution. EMBO J. *10*, 207–214.

Zamore, P. D., and Green, M. R. (1989). Identification, purification, and biochemical characterization of U2 small nuclear ribonucleoprotein auxiliary factor. Proc. Natl. Acad. Sci. USA *86*, 9243–9247.

Zamore, P., Patton, J., and Green, M. (1992). Cloning and domain structure of the mammalian splicing factor U2AF. Nature *355*, 609–614.

Zhang, M., Zamore, P. D., Carmo-Fonseca, M., Lamond, A. I., and Green, M. R. (1992). Cloning and intracellular localization of the U2 small nuclear ribonucleoprotein auxiliary factor small subunit. Proc. Natl. Acad. Sci. USA *89*, 8769–8773.

Zhang, M. Q., and Marr, T. G. (1994). Fission yeast gene stucture and recognition. Nucleic Acids Res. *22*, 1750–1759.

Zhang, W. J., and Wu, J. Y. (1996). Functional properties of p54, a novel SR protein active in constitutive and alternative splicing. Mol. Cell. Biol. *16*, 5400–5408.

Zhang, W. J., and Wu, J. Y. (1998). Sip1, a novel RS domain-containing protein essential for pre-mRNA splicing. Mol. Cell. Biol. *18*, 676–684.

Zhuang, Y., and Weiner, A. M. (1986). A compensatory base change in U1 snRNA suppresses a 5′ splice site mutation. Cell *46*, 827–835.

Zorio, D. A., Lea, K., and Blumenthal, T. (1997). Cloning of *Caenorhabditis* $U2AF^{65}$: an alternatively spliced RNA containing a novel exon. Mol. Cell. Biol. *17*, 946–953.

Zorio, D.A., and Blumenthal, T. (1999a). $U2AF^{35}$ is encoded by an essential gene clustered in an operon with RRM/cyclophilin in *Caenorhabditis elegans.* RNA *5*, 487–494.

Zorio, D., and Blumenthal, T. (1999b). Both subunits of U2AF recognize the 3′ splice site in *Caenorhabditis elegans.* Nature *402*, 835–838.

Zuo, P., and Maniatis, T. (1996). The splicing factor $U2AF^{35}$ mediates critical protein-protein interactions in constitutive and enhancer-dependent splicing. Genes Dev. *10*, 1356–1368.